JOURNAL OF Materials CHEMISTRY

Synthesis of Na-2-mica from metakaolin and its cation exchange properties

Tatsuya Kodama,*[a]† Takayuki Higuchi,[a] Tadaaki Shimizu,[b] Ken-ichi Shimizu,[b] Sridhar Komarneni,[c] Wilfried Hoffbauer[d] and Hartmut Schneider[e]

[a]*Department of Chemistry & Chemical Engineering, Faculty of Engineering, Niigata University, 8050 Ikarashi 2-nocho, Niigata 950-2181, Japan*
[b]*Graduate School of Science and Technology, Niigata University, 8050 Ikarashi 2-nocho, Niigata 950-2181, Japan*
[c]*Materials Research Laboratory and Department of Agronomy, The Pennsylvania State University, University Park, PA, 16802, USA*
[d]*Institute of Inorganic Chemistry, University of Bonn, D-53121 Bonn, Germany*
[e]*Ceramic Department, Institute of Materials Research, German Aerospace Research Establishment-DLR, D-51170 Köln, Germany*

Received 6th February 2001, Accepted 15th May 2001
First published as an Advance Article on the web 4th July 2001

Na-2-mica of the ideal composition of $Na_2Mg_6Al_2Si_6O_{20}F_4{\cdot}xH_2O$ was prepared from a mixture of NaF, magnesium nitrate, SiO_2 and calcined kaolinite (the latter serving as a cost-effective aluminosilicate source) at 800 °C and was found to excel in Sr removal from solutions at room temperature. This mica was characterized by powder X-ray diffraction (XRD), scanning electron microscopy (SEM) and ^{27}Al and ^{29}Si magic angle spinning nuclear magnetic resonance (MAS-NMR) spectroscopy. Fundamental studies of $nNa^+ \rightarrow M^{n+}$ ($M^{n+} = Sr^{2+}$, Ca^{2+}, Li^+, K^+ and Cs^+) equilibria revealed a high selectivity and large capacity for Sr^{2+} ion uptake. A relatively low-temperature heat treatment (200 °C) of the Sr-exchanged mica resulted in collapse of the hydrated interlayer spacings of the mica, which will be useful to immobilize strontium in the stable unhydrated phase. This selective Sr-ion exchanger is expected to be useful for ^{90}Sr removal and its immobilization.

Introduction

Numerous approaches and technologies have been developed and practiced for the disposal and immobilization of radioactive aqueous wastes generated at different stages of the nuclear fuel cycle.[1] The treatment process based on adsorption or ion exchange plays an important role in preconcentration and separation of toxic radionuclides from aqueous wastes.[1,2] A need exists for high performance cation exchangers to separate ^{90}Sr and ^{137}Cs from high-level alkaline tank wastes and remediation of process and ground water at the Hanford nuclear site, the latter to prevent contamination of the Columbia River.[3] Synthetic inorganic layered materials have been investigated extensively for the removal and fixation of ^{90}Sr and ^{137}Cs.[4–6]

Mica is one of the most representative of the 2 : 1 phyllosilicate clays, each layer consisting of an octahedral sheet sandwiched between two tetrahedral sheets, and is distinguished from smectites or vermiculites by their higher layer charge density. Due to the high layer charge density, naturally occurring micas do not swell in water, and as a result, ion exchange reactions with the interlayer cations do not easily occur. Synthetic micas, which swell in water, with cation exchange capacities of more than 200 mequiv $(100\ g)^{-1}$ have been prepared and these are of considerable interest.[7–19] In particular, the synthetic clay mineral "Na-4-mica" (ideal chemical composition $Na_4Mg_6Al_4Si_4O_{20}F_4{\cdot}xH_2O$) has the largest theoretical cation-exchange capacity of 468 mequiv $(100\ g)^{-1}$ on an anhydrous basis and readily becomes hydrated on contact with water or even in moist air at ambient conditions.[10–19] Paulus *et al.*[12] first reported that a very fine (1–5 μm in size) and pure phase of Na-4-mica could be prepared by a solution–sol–gel process. They further showed that the mica so produced had high cation-exchange selectivities for many divalent transition-metal ions and for strontium and barium, but not for the alkali-metal ions, and the alkaline earth ions magnesium and calcium.[13] This synthetic method, however, is not economical because of the use of expensive chemicals such as tetraethoxysilane and the long and tedious procedure. We previously reported a much more simple and cost-effective synthetic route for the synthesis of Na-4-mica which utilizes naturally occurring kaolinite as an inexpensive aluminosilicate source.[14–19]

Recently, we also reported the synthesis of another new swelling mica phase, $Na_2Mg_6Al_2Si_6O_{20}F_4{\cdot}xH_2O$ (hereafter referred to as "Na-2-mica") by the solution–sol–gel process and reported that this phase is also an excellent Sr ion exchanger.[20] A comparative study with existing Sr selective ion exchangers clearly revealed that this synthetic clay exhibited the best performance for ^{90}Sr removal from actual ground water collected from three different locations at Hanford.[20] In this work, we report the synthesis of Na-2-mica from kaolinite. We also report the cation exchange equilibria of $2Na^+ \rightarrow Sr^{2+}$ or Ca^{2+}, and $Na^+ \rightarrow Li^+$, K^+ or Cs^+ in this Na-2-mica at room temperature and show that this mica excels in Sr removal from solutions, as expected.

†Permanent address: Department of Chemistry & Chemical Engineering, Faculty of Engineering, Niigata University, 8050 Ikarashi 2-nocho, Niigata 950-2181, Japan. E-mail: tkodama@eng.niigata-u.ac.jp

 DOI: 10.1039/b101186n

This journal is © The Royal Society of Chemistry 2001

Experimental

Preparation of micas

Naturally occurring kaolinite has the theoretical chemical composition $Al_2Si_2O_5(OH)_4{\cdot}nH_2O$. A poorly crystallized kaolinite of composition, 47.9% SiO_2, 38.3% Al_2O_3, 2.08% TiO_2, 0.98% Fe_2O_3, 0.15% FeO and 0.03% MgO (supplied by Georgia Kaolin Company through W. D. Johns, Dept. of Geology, Univ. of Missouri, Columbia, MO 65201, USA), was used for the synthesis of the mica. Na-4-mica was previously prepared from a precursor mixture of NaF, magnesium nitrate and calcined kaolinite at 800 °C.[19] The original synthetic process for Na-4-mica is briefly outlined as follows. The poorly crystallized kaolinite was first calcined at 700 °C for 18 h to transform it to an amorphous product (on heating to around 600 °C, kaolinite is completely dehydrated and loses its crystalline character) which is the so-called metakaolin ($Al_2Si_2O_7$). The metakaolin was cooled and stored in a desiccator over silica gel at room temperature. Appropriate amounts of magnesium nitrate [$Mg(NO_3)_2{\cdot}6H_2O$] and the metakaolin were mixed to obtain a stoichiometric composition (Mg : Al : Si = 3 : 2 : 2). Then it was mixed with an equal mass of NaF, thoroughly homogenized using a pestle and mortar, and transferred to an alumina vessel. The precursor mixture was calcined for 24 h at 800 °C in air using a programmed furnace. The resulting solid was gently ground and washed in deionized water several times to remove excess NaF. Any remaining impurity phases, such as insoluble fluoride salts, were then removed with repeated washings using saturated boric acid solution.[12,14] Then, the solid was washed with 1 M NaCl solution three times to completely saturate all the exchange sites with Na^+. The product was finally washed with deionized water and dried at 60 °C in an oven for 2–3 days. The products thus prepared were stored in a desiccator over silica gel at room temperature.

In the present work, we attempted the synthesis of $Na_2Mg_6Al_2Si_6O_{20}F_4{\cdot}xH_2O$ by modification of this simple and cost-effective synthetic process from kaolinite. Thus, in the modified procedure, SiO_2, magnesium nitrate and the metakaolin was mixed in order to obtain the precursor mixture with the stoichiometric composition of Mg : Al : Si = 3 : 1 : 3. Then it was mixed with an equal mass of NaF, thoroughly homogenized using a pestle and mortar, and transferred to an alumina vessel. The precursor mixture was reacted for 24 h at 800 °C in air using a programmed furnace. The resultant solid thus prepared was gently ground, washed, Na^+-saturated, dried and stored by the same procedures as used above for the original synthetic process for Na-4-mica.

Characterization of products

Powder X-ray diffraction (XRD) was carried out to check for phase purity and to determine the basal spacings of the mica using a Rigaku RAD-γA diffractometer with CuKα radiation. Scanning electron microscopy (SEM) was used to determine the crystallite size and shape (EPMA-8705, Shimadzu). The metal oxide contents, sodium, aluminium, silicon, magnesium, iron and titanium oxide contents, were determined by lithium borate fusion and chemical analyses using atomic emission spectrometry (SpectraSpan III instrument). Water content was determined by thermal analysis. Magnetic-angle spinning NMR ^{27}Al and ^{29}Si spectra were obtained at 103.9 and 79.8 MHz respectively using a Varian Unity 400 spectrometer with a double bearing rotor (5 mm, zirconia).[17] For ^{27}Al resonance the spectrometer operating conditions were: pulse width 1 ms (equivalent to π/18 pulses, measured on $Al(NO_3)_3$ aqueous solution), spectral width 1 MHz, recycle delay 1.0 s, number of transients 2000, and spinning speed 12 kHz. No line broadening was considered in data processing.[17] Chemical shifts were measured relative to aqueous $Al(NO_3)_3$. The ^{29}Si spectra were acquired by using a 4 μs pulse width, 40 kHz spectral width, recycle delay of 60 s, 1000 transients, and 8 kHz spinning speed.[17] Line broadening of 10 Hz was used in data processing. Chemical shifts were referenced to the signal of tetramethylsilane (TMS).

Cation exchange isotherm determination

A 25 mg portion of the mica (anhydrous basis) was equilibrated with 25 cm^3 of the mixed solution having different mole ratios of Na^+/M^{n+} ($M^{n+} = Li^+$, K^+, Cs^+, Sr^{2+} and Ca^{2+}) with shaking at 25 °C for 4 weeks. The total normality of the solutions was kept constant at 0.00468 N. After equilibration, the supernatant solution was analyzed for the alkali-metal and alkaline earth metal ions by atomic emission spectroscopy. The amounts of metal ions exchanged by the mica were determined from the difference in the concentration between the sample solution and the reference. All these equilibria experiments were conducted in triplicate to check for reproducibility. The errors in the triplicates were about ±5%.

Theoretical

The theory for the cation exchange used in this work was described in our previous reports[15,16] and is outlined as follows. The cation exchange process between Na^+ and M^{n+} on the Na-rich mica is represented by,

$$n\overline{Na}^+ + M^{n+} \rightleftarrows nNa^+ + \overline{M}^{n+} \quad (1)$$

where the bar above the symbols represents the ion exchanger phase. The thermodynamic equilibrium constant, K, of the reversible ion-exchange reaction is defined by,

$$K = \frac{[Na^+]^n \overline{X}_M \gamma_{Na}^n f_M}{[M^{n+}] \overline{X}_{Na}^n \gamma_M f_{Na}^n} = K_{Na}^M \frac{f_M}{f_{Na}^n} \quad (2)$$

and

$$K_{Na}^M = \frac{X_{Na}^n \overline{X}_M \gamma_{Na}^n}{X_M \overline{X}_{Na}^n \gamma_M} [n(TN)^{n-1}] = \frac{(1-X_M)^n \overline{X}_M \gamma_{Na}^n}{X_M (1-\overline{X}_M)^n \gamma_M} [n(TN)^{n-1}] \quad (3)$$

where $[Na^+]$ and $[M^{n+}]$ are molalities of the ions in solution; X_i and $\bar{X}_i$ are the equivalent fractions of exchanging ion, i, in the solution phase and in the ion-exchanger phase, respectively; γ_i and f_i are activity coefficients in the solution and in the ion-exchanger, respectively; TN represents the total normality of the solution ($TN = [Na^+] + n[M^{n+}]$); and K_{Na}^M refers to the corrected selectivity coefficient. $\bar{X}_i$ is defined by

$$\overline{X}_{Na} = \frac{[\overline{Na}^+]}{n[\overline{M}^{n+}] + [\overline{Na}^+]} \qquad \overline{X}_M = \frac{n[\overline{M}^{n+}]}{n[\overline{M}^{n+}] + [\overline{Na}^+]} \quad (4)$$

$$[\overline{Na}^+] + n[\overline{M}^{n+}] = TC \quad (5)$$

where TC represents the theoretical or total capacity.

A corrected selectivity coefficient larger than unity ($\ln K_{Na}^M > 0$) indicates selectivity for the ion M^{n+}.[21] Na^+ ions are more preferred if K_{Na}^M is smaller than unity ($\ln K_{Na}^M < 0$). When K_{Na}^M is equal to unity ($\ln K_{Na}^M = 0$), no preference between these ions is indicated. The corrected selectivity coefficient, K_{Na}^M, is related to the Kielland coefficient as given below.[22,23] Kielland plots show the details of the ion exchange selectivity as a function of the equivalent fraction, $\bar{X}_M$. A plot of $\log K_{Na}^M$ *vs.* $\bar{X}_M$ (Kielland plot) is generally represented by the polynomial function[24]

$$\log K_{Na}^{M} = \sum_{m=1} (m+1) C_m \overline{X}_M^m + \log (K_{Na}^{M})_{X_M, \overline{X}_M \to 0} \quad (6)$$

where the coefficient, C_m, is called the generalized Kielland coefficient. The Kielland plots often give linear relationships with a slope $2C_1$, in which case eqn. (6) can become

$$\log K_{Na}^{M} = 2C_1 \overline{X}_M + \log (K_{Na}^{M})_{X_M, \overline{X}_M \to 0} \quad (7)$$

The generalized Kielland coefficient, C_1, is related to the energy term for the steric limitation or jumping barrier for the exchanging ions in the interlayer.[25] Generally, the C_1 value is a negative constant, depending on the ion exchanger system. This means that ion exchange becomes more difficult with progressive exchange. In this case, the energy term for the steric limitation is larger as the $|C_1|$ value is larger. The value of the intercept of the Kielland plot, $(K_{Na}^{M})_{X_M, \bar{X}_{M\to 0}}$, indicates the corrected selectivity coefficient at infinitesimal exchange (very small $\bar{X}_M$) which is very important for interpreting the chromatographic behavior of metal ions.

The K_d value is more useful in practical applications for interpreting the chromatographic behavior of metal ions. It is defined by,

$$K_d = \frac{[\overline{M}^{n+}]}{[M^{n+}]} = \frac{TC\overline{X}_M}{TNX_M} \quad (8)$$

Results and discussion

Characterization of Na-rich mica

The XRD pattern of the resultant solid prepared by the modified procedure, using the precursor mixture of metakaolin, magnesium nitrate, SiO_2 and NaF (Mg : Si : Al molar ratio = 3 : 1 : 3), is shown in Fig. 1. A strong peak was observed at $d = 12.11$ Å, which can be assigned to the (001) reflection of a hydrated fluorine mica with a single sheet of interlayer water.[10] Small peaks observed around $d = 6.07$, 4.01 and 3.04 Å are assigned to (002), (003) and (004) reflections of the c-axis spacing of the hydrated mica. This XRD pattern was almost the same as that of the hydrated Na-2-mica previously prepared by the solution–sol–gel process.[20]

The metal oxide and water contents of the mica prepared by the modified procedure are given in Table 1. The Si/Al molar ratio of the mica is 2.5 which is somewhat lower than that expected for Na-2-mica (Si/Al molar ratio = 3). The sodium content of the mica, however, is much higher than that expected for Na-2-mica. The Na : Al ratio expected for Na-2-mica is 1.0 but the observed Na : Al ratio is 1.8. This higher sodium oxide content would be due to the presence of some impurity phase. Thus, here we estimated the chemical composition of the mica phase from the aluminium, silicon and magnesium oxide contents, based on $O_{20}F_4$ as expected for 2 : 1 layer aluminosilicate, assuming that no cation vacancies are present in the tetrahedral sheets. Oxides of iron and titanium were not used in the calculation of formulae because these are not expected to substitute into the mica structure. The number of interlayer Na^+ ions in the chemical formula was estimated from the charge balance. This estimation gave the chemical composition of $Na_{1.98}Mg_{6.14}Al_{2.26}Si_{5.74}O_{20}F_4$ for the mica phase, which is very close to the ideal composition of Na-2-mica.

The ^{29}Si MAS-NMR spectrum of the Na-2-mica prepared by the modified procedure is presented in Fig. 2 and Table 2. The spectrum of the Na-2-mica showed quite a different pattern from that of the Na-4-mica which was previously reported.[17,18] Significant resonances appeared at δ −77.8, −82.4, −85.0 and −92.2, which can be assigned to Si(3Al), Si(2Al), Si(1Al) and Si(3Si) environments, respectively.[11,14,17,26] Compared to the Na-4-mica, the Si(2Al), Si(1Al) and Si(3Si) resonances are more intense, indicating that the Si/Al ratio in the tetrahedral sheets is increased in the Na-2-mica.

The ^{27}Al MAS-NMR spectrum of the Na-2-mica prepared by the modified procedure is shown in Fig. 3. There is no resonance due to Al in octahedral coordination, which should appear at around 0 ppm.[26] The spectrum shows a strong resonance due to Al in tetrahedral coordination at δ *ca.* 63.4 from $[Al(H_2O)_6]^{3+}$. Thus, this spectrum indicated that nearly all of the Al was incorporated in the tetrahedral sites. A shoulder resonance around 60 ppm was, however, observed, which represented a second Al tetrahedral environment. It is not clear at this point what this tetrahedral environment is, but

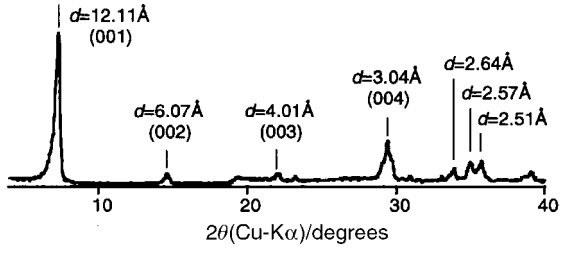

Fig. 1 XRD pattern of the mica prepared by the modified procedure using the precursor mixture of metakaolin, magnesium nitrate, SiO_2 and NaF (Mg : Si : Al molar ratio = 3 : 1 : 3).

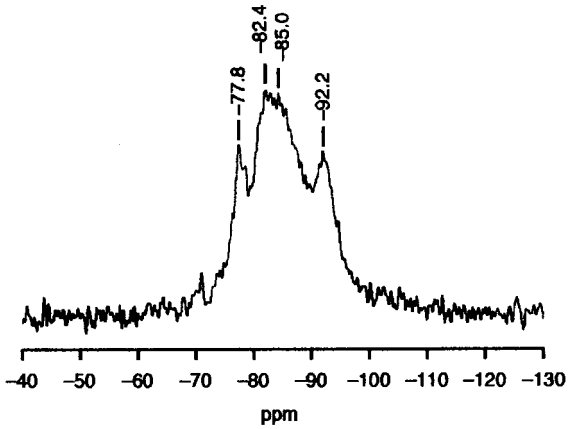

Fig. 2 ^{29}Si MAS-NMR spectrum (ref. TMS) of the Na-2-mica prepared by the modified procedure.

Table 1 Analytical data for Na-rich mica prepared by the modified synthetic process

Content[a]/wt%						
SiO_2	Al_2O_3	TiO_2	Fe_2O_3	MgO	Na_2O	H_2O[b]
35.2	11.8	0.66	0.33	25.3	12.8	12.5

[a]The metal oxide contents were determined by lithium borate fusion and chemical analyses using atomic emission spectrometry. [b]Determined by thermal analysis.

Table 2 ^{29}Si MAS-NMR data (chemical shift δ relative to TMS, and the normalized intensity I) for Na-2-mica

	Tetrahedral environments of Si[a]			
	Si(3Al)	Si(2Al)	Si(1Al)	Si(3Si)
δ	−77.8	−82.4	−85.0	−92.2
I(%)	22.2	29.1	27.5	21.2

[a]Assignment of the chemical shifts was based on refs. 11, 14, 17 and 27.

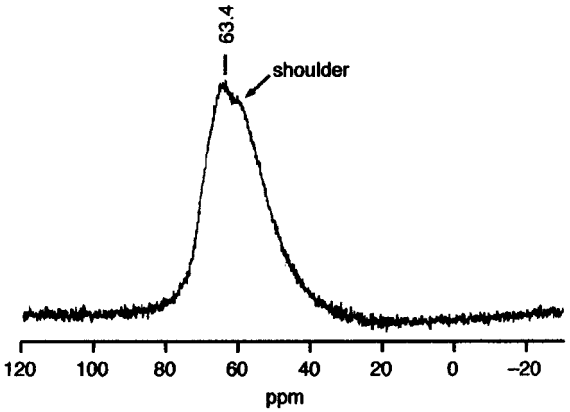

Fig. 3 ^{27}Al MAS-NMR spectrum (ref. $[Al(H_2O)_6]^{3+}$) of the Na-2-mica prepared by the modified procedure.

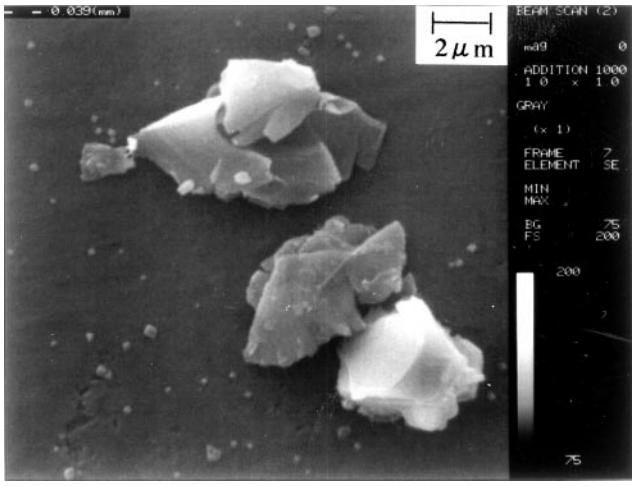

Fig. 4 SEM micrograph of the Na-2-mica prepared by the modified procedure.

this second Al tetrahedral environment has been frequently observed in the ^{27}Al MAS-NMR spectra of Na-4-micas.[17,18] Komarneni *et al.* previously concluded that the shoulder was probably due to the glassy impurity phase.[17] This impurity glassy phase must contain large amounts of sodium to increase the sodium content of the Na-2-mica here, as mentioned above. The fraction of the impurity phase must be very small because only a small shoulder resonance was observed at 60 ppm.

The SEM micrograph of the Na-2-mica is shown in Fig. 4, which shows plate-like and pseudo hexagonal crystallites of around 2–5 μm in size.

Cation exchange properties of the Na-2-mica

Fig. 5a shows the $2Na^+ \rightarrow Sr^{2+}$ and Ca^{2+} exchange isotherms with Na-2-mica: the theoretical CEC of 247 mequiv (100 g)$^{-1}$, based on the ideal chemical composition of Na-2-mica (on an anhydrous basis), was used for representing the isotherms. The Sr ion uptake at the *TN* of 0.00468 N reached 199 mequiv (100 g)$^{-1}$, which is 81% of the theoretical CEC. Under the same cation exchange reaction conditions, Na-2-mica prepared by the solution–sol–gel process attained an Sr ion uptake of 231 mequiv (100 g)$^{-1}$.[20] The Na-4-mica which was previously prepared by the same procedure from kaolinite at 800 °C exhibited a crystallite size of about 2–3 μm, which is almost the same as that of the Na-2-mica prepared in the present work.[19] The Sr ion uptake at $TN = 0.00468$ N with Na-4-mica reached only 83 mequiv (100 g)$^{-1}$.[19] The Ca ion uptake at $TN = 0.00468$ N with the present Na-2-mica reached 136 mequiv (100 g)$^{-1}$, which is about 55% of the CEC.

The Kielland plots for the Sr and Ca exchange reactions almost gave linear relations (Fig. 5b). This indicates that the cation-exchange reaction proceeds on one kind of exchangeable site of the mica,[24,25] which is the interlayer Na^+ site of Na-2-mica. Thus, it is considered that the sodium ions in the impurity phase scarcely contribute to the cation-exchange reaction. By fitting the experimental K^M_{Na} and corresponding $\bar{X}_M$ values to a linear equation, the Kielland coefficient C_1 and $\log(K^M_{Na})_{X_M.\bar{X}_M \rightarrow 0}$ values were calculated and are listed in Table 3. The dotted line in Fig. 5b indicates that the corrected selectivity coefficient is equal to unity. The Kielland plots for the Sr exchange fall above the dotted line at $\bar{X}_{Sr} < 0.32$, indicating that here Sr^{2+} ions are thermodynamically more preferred over Na^+. The Na-2-mica prepared earlier[20] by the sol–gel method had somewhat higher selectivity for Sr than the present mica prepared from kaolinite (see Fig. 2 in ref. 20). The impurity phase might be responsible for this decreased selectivity.

Fig. 6 shows the $Na^+ \rightarrow Li^+$, K^+ and Cs^+ exchange isotherms and their Kielland plots with Na-2-mica. The

Table 3 Metal ion uptake and thermodynamic data for $nNa^+ \rightarrow M^{n+}$ exchange on the Na-2-mica prepared by the modified procedure

Cation	Metal ion uptake[a]/ mequiv (100 g)$^{-1}$	$\bar{X}_M$ range	$\log(K^M_{Na})_{\bar{X}_M 60}$	C_1
Sr^{2+}	199	0.19–0.81	0.50	−0.78
Ca^{2+}	136	0.18–0.55	−0.08	−1.99
Li^+	26	0.11–0.13	—	—
K^+	111	0.11–0.44	0.71	−0.86
Cs^+	62	0.09–0.31	—	—

[a]Obtained for the initial metal concentration of 0.00468 equiv dm^{-3}.

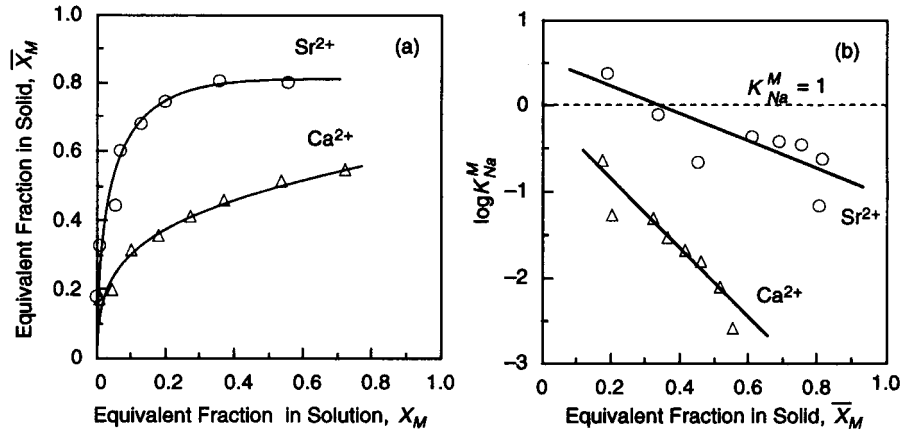

Fig. 5 Cation exchange isotherms (a) and Kielland plots (b) for $2Na^+ \rightarrow Sr^{2+}$ (○) and Ca^{2+} (△) exchange at room temperature with the Na-2-mica prepared by the modified procedure.

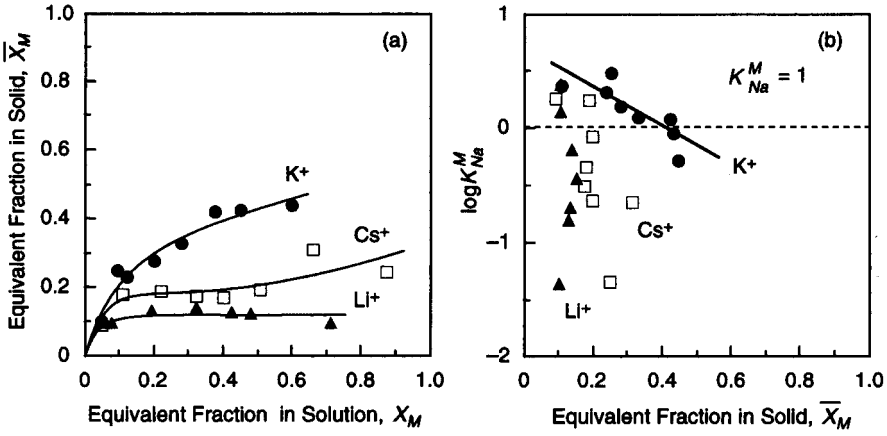

Fig. 6 Cation exchange isotherms (a) and Kielland plots (b) for $Na^+ \rightarrow Li^+$ (▲), K^+ (●) and Cs^+ (□) exchange at room temperature with the Na-2-mica prepared by the modified procedure.

thermodynamic selectivity increased in the order of $Li^+ < Cs^+ < K^+$.

The distribution coefficients (K_d) are more useful for practical applications. The K_d values were calculated using equation (8) and are plotted against $\bar{X}_M$ in Fig. 7. In the wide $\bar{X}_M$ range, the K_d values for Sr^{2+} were much higher than those for Ca^{2+}, K^+, Cs^+ and Li^+.

The Sr-exchanged mica with the $\bar{X}_{Sr}$ of 0.81 was heated to collapse the interlayers by dehydration. Fig. 8 shows the change in XRD peaks for the (001) reflection of the Sr-exchanged mica with and without heat treatment. The basal spacing decreased from 12.28 to 9.99 Å by heating at 200 °C, indicating that the hydrated interlayer spacings collapsed and the mica turned into the unhydrated phase. Partial interlayer collapse occurred at 150 °C (Fig. 8b) as indicated by the smaller 9.99 Å peak. It is expected that collapse of the hydrated interlayer region leads to effective strontium fixation, as the strontium becomes trapped into a more conventional trioctahedral brittle mica structure similar to the barium interlayered mica, kinoshitalite, $Ba_2(Mg,Mg,Al)_6Si_4Al_4O_{20}(OH,F)_4$, which is an extremely stable phase because the high coulombic forces that span the interlayer region effectively hold it very tightly closed.[27]

Conclusions

The swelling Na-2-mica was synthesized by the crystallization of a precursor mixture of calcined kaolinite, magnesium nitrate, SiO_2 and NaF flux at 800 °C. This cation exchanger showed a much higher selectivity for Sr than for Ca, K, Cs and Li. The Sr ion uptake reached 199 mequiv (100 g)$^{-1}$ even at a low initial Sr^{2+} concentration of 0.00468 N, which was much larger than that achieved for Na-4-mica with similar crystallite size. The interlayer spacings of the Sr-exchanged mica collapsed upon the relatively low-temperature treatment at 200 °C, which is expected to result in low Sr leachability from the Sr-exchanged mica. This selective Sr-ion exchanger is expected to be useful for the decontamination of the environment after accidental release and contamination with ^{90}Sr.

Acknowledgements

This research was supported by the Interfacial, Transport and Separation Process, Division of Chemical and Transport Systems, National Science Foundation under Grant No. CTS-9911580.

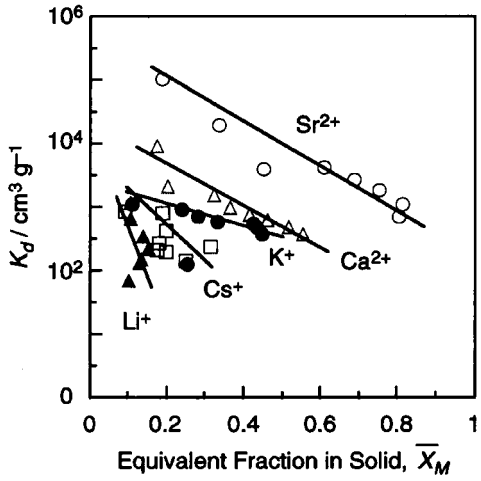

Fig. 7 Change in distribution coefficient (K_d) as a function of equivalent fraction of metal ion in the mica ($\bar{X}_M$) for the $Na^+ \rightarrow Li^+$ (▲), K^+ (●) and Cs^+ (□) exchange and the $2Na^+ \rightarrow Sr^{2+}$ (○) and Ca^{2+} (△) exchange.

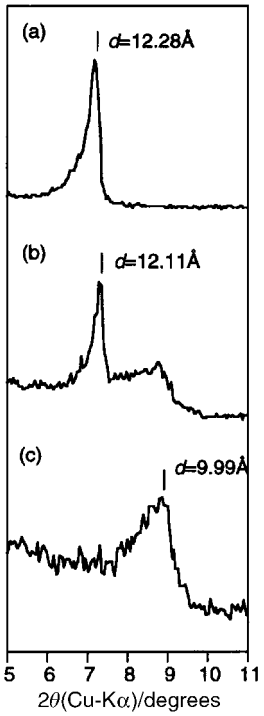

Fig. 8 Changes in XRD peak for the (001) reflection of the Sr-exchanged Na-2-mica with the $\bar{X}_{Sr}$ of 0.81 by heat treatment. (a) Original Sr-exchanged micas, (b) heat-treated at 150 °C and (c) heat-treated at 200 °C.

References

1 G. J. McCarthy, W. B. White, D. K. Smith and A. C. Lasaga, in *Radioactive Waste Disposal, Vol. 1: The Waste Package*, ed. R. Roy, Pergamon Press, New York, 1982, p. 72.
2 J. M. Kerr, *Bull. Am. Ceram. Soc.*, 1954, **38**, 374.
3 K. O'Donnell, *NBC News Story*, 1998, July 9.
4 S. Komarnani and R. Roy, *Science*, 1988, **239**, 1286.
5 J. Lehto, R. Harjula and A.-M. Girard, *J. Chem. Soc., Dalton Trans.*, 1989, 101.
6 A. Dyer, M. Pillinger, R. Harjula and S. Amin, *J. Mater. Chem.*, 2000, **10**, 1867.
7 Y. Morikawa, T. Goto, Y. Moro-oka and T. Ikawa, *Chem. Lett.*, 1982, 1667.
8 H. Sakurai, K. Urabe and Y. Izumi, *J. Chem. Soc., Chem. Commun.*, 1988, 1519.
9 J. W. Johnson, J. F. Brody, R. M. Alexander, L. N. Yacullo and C. F. Klein, *Chem. Mater.*, 1993, **5**, 36.
10 M. Gregorkiewitz and J. A. Rausell-Colom, *Am. Mineral.*, 1987, **72**, 515.
11 C. P. Herrero, M. Gregorkiewitz, J. Sanz and J. M. Serratosa, *Phys. Chem. Miner.*, 1987, **15**, 84.
12 W. J. Paulus, S. Komarneni and R. Roy, *Nature (London)*, 1992, **357**, 571.
13 S. Komarneni, W. J. Paulus and R. Roy, in *New Development in Ion Exchange; Proc. Int. Conf. Ion Exchange*, ed. M. Abe, T. Kataoka and T. Suzuki, Kodansha, Tokyo, 1991, p. 51.
14 S. Komarneni, R. Pidugu and J. E. Amonette, *J. Mater. Chem.*, 1998, **8**, 205.
15 T. Kodama and S. Komarneni, *J. Mater. Chem.*, 1999, **9**, 533.
16 T. Kodama and S. Komarneni, *J. Mater. Chem.*, 1999, **9**, 2475.
17 S. Komarneni, R. Pidugu, W. Hoffbauer and H. Schneider, *Clays Clay Miner.*, 1999, **47**, 410.
18 T. Kodama, S. Komarneni, W. Hoffbauer and H. Schneider, *J. Mater. Chem.*, 2000, **10**, 1649.
19 T. Kodama and S. Komarnani, *Sep. Sci. Technol.*, 2000, **35**, 1133.
20 S. Komarneni, T. Kodama and W. J. Paulus, *J. Mater. Res.*, 2000, **15**, 1254.
21 F. Helfferich, *Ion Exchange*, Daver, New York, 1995, p. 170.
22 J. Kielland, *J. Soc. Chem. Ind. (London)*, 1935, **54**, 232T.
23 G. L. Gaines Jr. and H. C. Thomas, *J. Chem. Phys.*, 1953, **21**, 714.
24 R. M. Barrer, *Natural Zeolites, Occurrence, Properities, Use*, ed. L. B. Sand and F. A. Mumpton, Pergamon, New York, 1978, p. 385.
25 R. M. Barrer and J. D. Falconer, *Proc. R. Soc. London A*, 1956, **236**, 227.
26 J. Sanz and J. M. Serratosa, *J. Am. Chem. Soc.*, 1984, **106**, 4790.
27 S. Guggenheim, in *Reviews of Mineralogy, Vol. 13, Micas*, ed. S. W. Bailey, Mineralogical Society of America-Bookcrafters. Inc., Chelsea, Michigan, 1984.